

## **Study on the cracking of carbon anodes used in aluminum industry**

Salah Amrani,<sup>1</sup> Duygu Kocaefe,<sup>1</sup> Yasar Kocaefe,<sup>1</sup> Dipankar Bhattacharyay,<sup>1</sup> Mohamed Bouazara,<sup>1</sup> Jules Côté<sup>2</sup>

<sup>1</sup>UQAC Research Chair on Industrial Materials (CHIMI), Aluminium Research Centre (REGAL), University of Québec at Chicoutimi, Chicoutimi, Québec, Canada

<sup>2</sup>Aluminerie Alouette Inc., Sept-Îles, Québec, Canada

### **Correspondence**

Duygu Kocaefe, UQAC Research Chair on Industrial Materials (CHIMI), Aluminium Research Centre (REGAL), University of Québec at Chicoutimi, Chicoutimi, Québec, Canada.

Email: Duygu\_Kocaefe@uqac.ca

### **Abstract**

Carbon anodes are used in aluminum electrolysis. Their quality plays a major role in the stability of cell operation and energy consumption. The improvement of the quality of carbon anodes is essential to respond to the many challenges the aluminum industry is facing with respect to issues related to carbon loss, energy use, cell performance, and production cost, especially for high amperage cells. The presence of cracks increases the anode resistivity, and, as a result, power consumption, production cost, and greenhouse gas emissions also increase. Therefore, it is important to know how the cracks form during anode production. An industrial measurement campaign was carried out at the Aluminerie Alouette Inc. (AAI) plant in Sept-Îles, Quebec, Canada. The effect of raw materials (type of coke, pitch, and butts), vibro-compaction (vibro-compactor type, balloon pressure, and vibration time), and the position of anodes in the baking furnace on anode cracking was investigated. It was found that the anode centre is the region that contains the most cracks compared to other parts of the anode. The cracks in the horizontal direction are more predominant than those in other directions. The raw materials and the operating parameters of each anode production step affect anode cracking.

### **KEYWORDS**

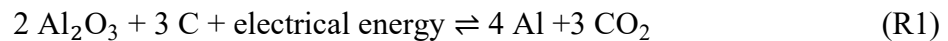
carbon anode production, anode cracking, vibro-compaction, baking, aluminum electrolysis

## 1 INTRODUCTION

Canada is the third largest aluminum producer in the world after China and Russia and is ranked second after Russia in aluminum exports. The aluminum industry is an important manufacturing industry, especially for Quebec, which accounts for nearly 90% of the total Canadian production. Of the nine smelters in Canada, eight are in Quebec and one is in British Columbia.<sup>[1-3]</sup>

Reduction in cost, energy consumption, and environmental emissions, along with increase in productivity, are identified as the most important challenges that the aluminum industry is facing today.<sup>[1]</sup> These challenges are strongly linked to the quality of carbon anodes. Increasing demand for high anode quality and adverse impact of certain aspects of the process on environment (gaseous emissions) combined with technological challenges to increase amperage, which has already reached around 600 kA, preoccupy the industry.

Aluminum is produced by the electrolysis of alumina using the Hall-Héroult process according to the reaction shown below:



Carbon anodes used for the electrolysis are made from petroleum coke, butts (top part of the anode which is not consumed during electrolysis, and thus recycled), rejected green and baked anodes (dry aggregate), and coal tar pitch. These are mixed (anode paste), compacted (green anode), and baked (baked anode) to produce the anodes that can be used in electrolysis after rodding.<sup>[4]</sup> Anode density is an important parameter in aluminum production, especially in high amperage cells. High density anodes have lower resistivity, longer life, and require less pitch; thus, they have reduced cost and increased productivity. The specific electrical resistance of the anode is also a key variable to lower the energy consumption. The carbon loss is linked to the operational practices (such as current efficiency), but also to anode reactivity with CO<sub>2</sub> and air. All of these have a direct impact on reducing cost and environmental emissions.

One major problem with high density anodes is the cracking.<sup>[5]</sup> The raw materials used and the anode fabrication parameters influence the anode properties.<sup>[4-8]</sup> Many factors during anode fabrication may contribute to stress build-up and cause thermal or mechanical shock, which results in the formation of cracks. Mixing (mixing time, energy, temperature, etc.),<sup>[4, 5, 9]</sup> vibro-compaction (paste temperature, forming temperature, vibration time, etc.),<sup>[5, 10-12]</sup> and baking parameters (heating rate, maximum temperature, maintenance time, position of anodes in the

furnace, temperature gradient, etc.)<sup>[4, 13-16]</sup> affect the anode quality and cracking. Cracks develop in over-compacted anodes whereas under-compacted anodes become too porous. At low temperatures, pitch becomes liquid and goes through expansion, which allows the release of stresses accumulated during forming and cooling of green anode (up to about 200°C) followed by its redistribution within the matrix due to its expansion (150-300°C). After, the volatiles are released as a result of the carbonization reactions (200-600°C), and the pitch changes from plastic to solid matrix due to coking (450-600°C).<sup>[17]</sup> During this period, many thermo-mechanical changes occur, which may result in crack formation. When the heating rate is high, the volatilization is too rapid. Then, the gas (volatile) pressure build-up leads to crack formation.<sup>[4, 5]</sup> Also, the non-uniform temperature distribution in the baking furnace and large temperature gradients in anodes can cause cracking.<sup>[18, 19]</sup>

There is a need for a comprehensive study to understand how the cracks form so that the modifications required in the anode preparation and baking operations can be identified. The carbon group at the University of Quebec at Chicoutimi (UQAC) carried out a number of studies on crack formation both in the laboratory and in the plant.<sup>[12, 19]</sup> In this article, the results of a measurement campaign in the plant are presented. The effect of raw materials (coke, pitch, and butts), vibro-compaction (vibro-compactor type, compaction time, and balloon pressure) and baking (placement of anodes in the furnace) parameters were investigated.

## **2 MATERIALS AND METHODS**

An industrial measurement campaign was carried out to study the effect of different parameters on cracking. First, 24 baked anodes were produced and cored. Then, the anodes were characterized to determine their properties such as apparent density, electrical resistivity, and crack density.

### **2.1 Anode production**

Industrial anodes were produced in the AAI plant. Figure 1 and Table 1 show the production conditions for these anodes. The same anode recipe was used for all the anodes of this study.

#### **2.1.1 Preparation of anode paste**

First, the coke, butt, and rejected anodes (aggregate) were prepared according to desired particle size distribution (anode recipe). It is important to have this distribution since the large particles give the anode mechanical strength whereas the small particles fill the voids in the coke bed,

leading to good anode properties. Then, the aggregate was mixed with pitch in a kneader around 170°C to produce the anode paste.<sup>[4]</sup>

### **2.1.2 Vibro-compaction**

The anode paste was compacted in a vibro-compactor to obtain green anodes. The details of vibro-compaction are given elsewhere.<sup>[12]</sup> The study involved 24 anodes manufactured using four vibro-compactors (V1, V2, V3, V4). Six anodes were produced by each vibro-compactor. Three of these six anodes were compacted using a vibration time of 30 seconds and the other three anodes were compacted for 37 seconds, as shown in Figure 1. Figure 1 also indicates the vibro-compactor used for each anode placed in two different pits of the baking furnace.

### **2.1.3 Baking**

The anodes were baked in a horizontal anode baking furnace. Figure 2 presents an overview of this type of furnace.<sup>[15]</sup> In this furnace, the anodes are placed in the pits and they are covered with packing coke to support the anodes and prevent their oxidation. Each pit is surrounded by two flues in which the gas flows. The flues contain baffles and spacers to ensure the uniform distribution of gas.<sup>[15, 20]</sup> The anodes are baked with the heat transferred from the hot gases in flues to the pits through the brick wall. The detailed information on the operation of the furnace is given elsewhere.<sup>[16]</sup>

Anodes produced with the compaction time of 30 seconds were baked in one pit of the baking furnace while those produced with the compaction time of 37 seconds were baked in another pit (Figure 1). The vibro-compactor (V1, V2, V3, or V4) used for each anode placed in one of the pits is also shown in Figure 1. As can be seen from Figure 1, the anodes formed in the same vibro-compactor were placed in the same position in both pits. Each pit contained three rows of six anodes. The unmarked positions contained anodes which were not used during this study. Figure 3 presents the placement of anodes in the pits with the given anode numbers. After baking, the anodes were visually inspected to see the types and positions of the cracks formed.

### **2.1.4 Visual inspection of the anodes for surface cracks**

A visual inspection of each anode is carried out to determine the anodes to be rejected. The test anodes were visually examined after baking to identify the position of different types of cracks developed on the anode surfaces.

## **2.2 Anode coring**

The anodes were cored, and twenty-five cores per anode were drilled during this study. The height of the cores was equal to the height of the anode. The positions of the cores in the anodes are given in Figure 4. Since these cores come from the inside of the anode, their surface cracks represent the internal anode cracks.

The characterization of the cracks present in the cores was carried out by visual inspection in order to identify the types of the cracks present and their positions in the test anodes. Cracks are classified according to following criteria.

#### **2.2.1 Classification of cracking in the horizontal direction in anodes**

The anodes were divided into three parts as right, middle, and left sides (Figure 4): the cores 11, 12, 13, 14, 15, 16, and 17 were on the right side; the cores 1, 2, 3, 4, 5, 6, 7, 8, 9, and 10 were in the middle; and the cores 18, 19, 20, 21, 22, 23, 24, and 25 were on the left side of the anodes.

#### **2.2.2 Classification of cracking in the vertical direction in anodes**

The cores were divided equally into three regions which represent the bottom, middle, and top parts of the anode in the vertical direction, respectively (Figure 5A).

#### **2.2.3 Classification of cracking according to crack type**

Cracks were also classified according to their type, namely, horizontal, vertical, and inclined (Figure 5B).

### **2.3 Determination of crack density**

The cracks were counted on each core. The crack density of each core was calculated from the ratio of the number of cracks to the corresponding area (lateral surface area of the core). The averages of the crack density in different sections of the anode (right, centre, and left or top, middle, and bottom) were determined by taking the average of the crack densities of the cores present in a given anode section. The relative crack density is calculated with respect to their mean values.

### **2.4 Measurement of apparent density and electrical resistivity**

The apparent density of cores was measured according to ASTM D5502-00 (2005), and their electrical resistivity was measured according to ASTM D6120-97 (2007).

## **3 RESULTS AND DISCUSSION**

### **3.1 Characterization of surface cracking by visual inspection of whole anodes**

Before coring the anodes, the surfaces of all the anodes were inspected visually. Figure 6 illustrates the different types of surface cracks (vertical and horizontal) that can develop on the surface of the anodes.

Crack type 1 developed in the stub holes. Crack type 2 was only seen in the central stub hole. Crack types 4, 6, and 7 were detected at the corners, towards the middle of the anode, and in the lower part of the corners, respectively. Crack types 3 and 5 (horizontal cracks) were present near the edges and in the middle of the anodes which were baked in row 1 (top of the pit). The horizontal cracks increase the electrical resistivity since they are perpendicular to the direction of the current. Crack type 2 was detected mainly in the anodes that were baked in row 3 (bottom of the pit). The other crack types (1, 4, 6, and 7) were randomly located in the anodes baked in different rows.

Figure 7 presents the percentage of surface cracks (the number of cracks found in the anodes of each vibro-compactor at a given vibration time relative to the total number of cracks found in all the anodes) formed during the compaction of test anodes at two different vibration times. The lowest percentage of cracking was found in the anodes produced by V3 with a vibration time of 30 seconds and those manufactured by V1 with 37 seconds. The anodes manufactured by V4 with 30 seconds vibration time had the highest number of cracks. The anodes made by V1 and V4 contained more cracks at 30 seconds than at 37 seconds. The reverse tendency was seen for vibro-compactors V2 and V3.

The percentage of surface cracks are shown in Figure 8 without taking the vibration time into account. V4 produced anodes with the highest number of cracks while V1 produced the anodes with the least number of cracks. These results represent only the problem of surface cracking of the test anodes. It is therefore difficult to determine the quality of the anodes based solely on the visual inspection of the surface. The inspection of cores gives more details on the internal cracking of the anodes.

During the visual inspection, a number of cracked stub holes were observed (Figure 9). Anodes have three stub holes. The one on the anode number side is identified as stub hole 3.

The results of the visual inspection of stub holes are shown in Figure 10. At the compaction time of 30 seconds, the results show that the problem of the cracked stub holes was observed for all the anodes produced with all vibro-compactors except V1. However, only the anodes produced with V3 had damaged stub holes when the vibration time was 37 seconds. Also, the number of

cracked stub holes was higher for V3 at 37 seconds. This might be due to the utilization of higher pressure in V3 (Table 1). Problems with cracked stub holes are likely to have a significant impact on current distribution in an anode, and thus on the energy consumption, due to the poor contact between the anode and the cast iron during rodding.<sup>[21]</sup>

### **3.2 Characterization of internal cracking by visual inspection of cores**

The baked carrots were characterized by visual inspection. The results are presented below.

#### **3.2.1 Distribution of the crack density in the horizontal direction in anodes**

Average crack densities for left, centre, and right sides of the anodes were calculated from the number of cracks observed on the surfaces of the cores coming from the corresponding parts as defined in Figure 4. Figure 11 presents the crack distribution for all baked anodes. It can be clearly seen from this figure that the cracking was most prominent at the centre of the anode. This might be due to stresses formed during the compaction of the stub holes. These stresses are released during the first phase of baking (up to 200°C), which results in cracking. There seems to be more cracking when high pressure was used (Table 1). The right and left sides of the anode had similar cracking densities. Also, the volatiles released during the second phase of baking (200-600°C) from the centre section of the anode have longer diffusion paths compared to those released from the side sections. This may have resulted in gas pressure build-up leading to more cracking.

#### **3.2.2 Distribution of the crack density in the vertical direction in anodes**

Figure 12 shows the distribution of cracks along the height of the anodes. The results show that the middle part of the anodes had a higher crack density compared to the top and bottom parts of the anodes. This again can be explained with the higher stresses formed in the region under the stub holes during the vibro-compaction which are released during the first phase of baking (up to 200°C) and the pressure build-up due to the volatile release during the second phase of baking (200-600°C). Also, the bottom of the anode had the lowest crack density. This might be due to the presence of slots which cover the entire length of the anode. They facilitate the evacuation of volatiles, resulting in less accumulation of pressure created by the volatile release.

#### **3.2.3 Distribution of the crack density according to crack type**

The visual inspection of the cores showed the presence of three types of cracks (horizontal, vertical, and inclined) in baked carbon anodes (Figure 5B). The distribution of the crack density according to crack type is shown in Figure 13. It was found that the vertical cracking was almost

negligible compared to others. The horizontal cracks were the most predominant. These types of cracks increase the electrical resistivity of the anode, consequently increasing the power consumption during electrolysis

### **3.2.4 Effect of anode position in the furnace**

It can be seen from Figure 13 that no matter which row in the furnace the anode was placed in, the number of vertical cracks was very small (light gray). The majority of cracks were horizontal (medium gray). There were also some inclined cracks (black).

Figure 14 presents the results for the effect of anode position in the furnace on the crack formation. The positions of anodes in the baking furnace are shown in Figures 1 (with the vibro-compactator used) and 3 (with anode numbers). The anodes baked in row 1 (top row, anodes 3, 4, 7, 10 at compaction time of 30 seconds and anodes 15, 16, 19, 23 at compaction time of 37 seconds, see Figure 13) of the furnace had the highest crack density. The anodes baked in row 3 (bottom row, anodes 2, 5, 9, 11 at compaction time of 30 seconds and anodes 13, 17, 20, 22 at compaction time of 37 seconds, see Figure 13) cracked the least. As can be seen from the results, the trend was similar at both vibration times. The cracking increased with increasing vibration time, but the trend remained the same. It was also observed that the temperatures at the top and the bottom of the furnace were similar. Therefore, the observed trend cannot be attributed to a greater temperature gradient in the top row. It seems that the charge on the anodes is the key parameter affecting cracking. The anodes placed in the bottom row (row 3) had two anodes placed on top of them (anodes placed in the second and third rows); consequently, they were subjected to a charge of approximately 2 tonnes (about 1 tonne/anode) while the anodes placed in the middle row (row 2) had a charge of about 1 ton since each supported only one anode placed in row 1. The anodes at the top (row 1) did not have any charge. The cracking was approximately uniform for a given row at a given vibration time, with the exception of anodes formed in V3 with higher vibration time. Balloon pressure during the forming of anodes in V3 were higher, which might be the cause of higher crack density of these anodes.

### **3.3 Effect of raw materials on cracking**

The results of this part were analyzed using the statistics since only two cokes, two pitches, and two butt concentrations were used, and more than one parameter was changed for each anode at a given time. Thus, two essential parameters of this method are:



- F-value is used in the analysis of variance (ANOVA). Variance is a measure of scatter in a data set. F-value is the ratio of two variances: the variance between the data sets to the variance in the same data set. The higher the F-value, the greater the chance that the variable studied will have a statistically significant effect. The F test gives F-value and F-critical value. If  $F\text{-value} > F\text{-critical value}$ , the parameter has a significant effect.
- p-value is an index of the reliability (significance) of a result. The lower the p-value is, the better the relation found between the variables is. Usually if  $p < 0.05$ , the parameter has a significant effect.

### 3.3.1 Butt content

Anodes were made using two different butt contents (Table 1). The results are presented in Figure 15. The results show that there is a small difference in crack density due to anode butt content, but the difference is not significant based on p-value as well as the comparison of f-value and F-critical value. However, the average value of the crack density indicates that the crack density increased when the amount of butts was increased. Butts are hard and non-porous. The difference between the mechanical properties of the butts and the fresh coke can cause cracking during baking.<sup>[4]</sup> Therefore, anodes with high butt content might be more prone to cracking.

### 3.3.2 Type of pitch

The properties of pitches are presented in Table 2. The effect of pitch type on crack density is shown in Figure 16. Based on the statistical analysis, the effect of pitch type on crack density is not statistically significant. However, the average values show that the effect of pitch 1 is more pronounced than that of Pitch 2. Pitch 1 has higher viscosity as well as lower  $\beta$ -resin and coking value compared to those of Pitch 2 (Table 2). Lower viscosity facilitates the penetration of pitch into the pores of coke. Therefore, the pitch distribution may be more uniform with Pitch 2. This pitch also has higher  $\beta$ -resin and coking value. If we assume that the volatile contents of pitches used in plants are usually similar (data not available), a larger percentage of Pitch 2 carbonizes and stays in coke while more volatiles are released during the coking of Pitch 1. This might be the cause of slightly higher crack density when Pitch 1 was used.

### **3.3.3 Coke**

Similarly, the effect of coke type on crack density was found to be not statistically significant (Figure 17). Based on the average values, anodes made with Coke 1 had a slightly higher crack density. The properties of cokes are shown in Table 3. The property of coke that most affects the crack formation is the grain hardness. Unfortunately, this data was not available. It is hard to relate the cracking to impurity content (reactivity) since some impurities are higher in Coke 1 and others are higher in Coke 2. It is known that Coke 2 was less porous even if exact porosities were not available. Since the same percentage of pitch was used for all the anodes, anodes made with Coke 1 might have been slightly under-pitched, since the pitch penetrates into the pores, leaving less amount of pitch around the particles. Therefore, cracks have probably formed between the particles since they were not fully bound. It must be noted from Table 1 that Coke 1 was always used with Pitch 1 and Coke 2 was always used with Pitch 2. Therefore, it is difficult to separate their effects on cracking.

### **3.4 Anode properties**

The average anode densities, electrical resistivities, and crack densities were calculated. The average of any property of an anode was determined from the average values measured for the 25 cores of each anode. The relative anode properties with respect to their mean values are presented in Table 4.

All the anodes had relatively high densities with the exception of anodes 16 and 18. Anode 19 had the highest anode density and crack density. It also had a high resistivity. This anode was compacted at high pressure with a longer compaction time in V3 and baked in row 1. This shows that high density anodes have cracks due to the stress accumulated during formation, and that they release these stresses during the first phase of baking. Also, during the volatile release phase, more gas pressure accumulates in dense anodes, which also causes more cracking. Figure 18 shows that the increasing resistivity indicates increased crack density.

## **4 CONCLUSIONS**

An industrial measurement campaign on the quality of anodes was carried out. The test anodes were manufactured using different raw materials and under various conditions. The surface cracks were studied by visually inspecting the surfaces of the anodes. The analysis results indicated that there are three types of surface cracks that can develop in dense anodes: horizontal,

vertical, and inclined. The results also showed that the horizontal type is predominant with a preferential localization in the middle of the anode and in the part, which is in the region of the surface below the stud holes. This type of crack increases the electrical resistivity.

Internal cracks were studied by coring the anodes and visually inspecting the core surfaces.

Concerning the raw materials, the utilization of excess butts, pitch with lower coking value, and coke with high porosity (if under-pitched) can contribute to anode cracking. During green anode formation, increasing the vibration time and balloon pressure led to an increase in crack growth.

In the baking stage, which is a critical step for the crack formation, position of anodes in the furnace affects the anode cracking. Baking anodes in the top row (row 1) of the furnace with no applied charge resulted in the highest anode crack density, whereas the anodes baked in row 3 with the highest applied charge gave the lowest crack density.

Anode making involves different steps, each of which have a number of operating parameters.

Each of these parameters can play a role in anode cracking. In this study, the effects of a number of parameters on cracking were investigated. However, plants have a large amount of data. A thorough analysis of these data may help better comprehend the overall picture.

## **ACKNOWLEDGEMENTS**

The technical and financial support of Aluminerie Alouette Inc. as well as the financial support of the Natural Sciences and Engineering Research Council of Canada (NSERC), Développement économique Sept-Îles (DESI), the University of Québec at Chicoutimi (UQAC), and the Foundation of the University of Québec at Chicoutimi (FUQAC) is greatly appreciated (Grant number: RDCPJ 417499-11).

## **REFERENCES**

- [1] Canadian Primary Aluminium Production ,(Aluminium Association of Canada, 2017), <https://www.aluminum.org/sites/default/files/CanadaPrimaryProduction092017.pdf>, Accessed 8 September 2020
- [2] Stratégie québécoise de développement de l'aluminium 2015-2025. (Government of Quebec, 2015), <https://www.quebec.ca/gouv/ministere/economie/publications/strategie-quebecoise-de-developpement-de-laluminium-2015-2025/>, Accessed 8 September 2020

- [3] L'avenir prend forme. (Government of Quebec, 2015),  
[https://www.economie.gouv.qc.ca/fileadmin/contenu/publications/administratives/strategies/strategie\\_aluminium.pdf](https://www.economie.gouv.qc.ca/fileadmin/contenu/publications/administratives/strategies/strategie_aluminium.pdf), Accessed 8 September 2020
- [4] K. I. Hulse, Anode Manufacture, *Raw Materials Formulation and Processing Parameters*, R&D Carbon Ltd., Sierre, Switzerland, **2000**, p. 63.
- [5] M.W. Meier, *Cracking, Cracking Behaviour of Anode*, R&D Carbon Ltd., Sierre, Switzerland, **1996**, p. 251.
- [6] K. Azari, Alamdari, H., G. Aryanpur, D. Ziegler, D. Picard, M. Fafard, *Powder Technol*, **2013**, 246, 650.
- [7] F.E.O. Figueiredo., C.R. Kato, A.S. Nascimento, A.O.F. Marques, P. Miotto, *Light Metals*, **2005**, 665.
- [8] S.S. Zhuchkov, S.A. Khramenko, presented at the Second International Congress on Non-Ferrous Metals, Krasnoyarsk, September **2010**.
- [9] S. Yi, G. Huai, Z. Shanhong, L. Chaodong, X. Haifei, *Light Metals*, **2013**, 1127.
- [10] P.H. Jonathan, B. Arnaud, T. Sonia, 10th Australasian Aluminium Smelting Technology Conference, Launceston, October **2011**.
- [11] K.A. Dorcheh, Ph.D. Thesis, Laval University, Quebec, Canada **2013**.
- [12] F. Rebaine, Ph. D. Thesis, University of Quebec at Chicoutimi, Quebec, Canada **2015**.
- [13] F. Keller, *Importance of baking technology on anode quality, Anode for the aluminum industry*, 2nd edition, R&D Carbon Ltd., Sierre, Switzerland, **2006**, p. 223.
- [14] M. Tkac, Ph.D. Thesis, Norwegian University of Science and Technology, Norway **2007**.
- [15] F. Keller, P.O. Sulger, *Anode baking; Baking of anodes for the aluminum industry*, 2nd edition, R&D Carbon Ltd., Sierre, Switzerland, **2009**, p. 223.
- [16] M. Baiteche, Ph. D. Thesis, University of Quebec at Chicoutimi, Quebec, Canada **2015**.
- [17] J. Hurlen, T. Naterstad, *J. Met.*, 43(11), **1991**, p. 20-25.
- [18] W.K. Fischer, F. Keller, R.C. Perruchoud, S. Oderbolz, *Light Metals*, **1993**, p. 683.
- [19] S. Amrani, Ph. D. Thesis, University of Quebec at Chicoutimi, Quebec, Canada **2015**.

- [20] A. Charette, Y. Kocaefe Y., D. Kocaefe D., *Le Carbone dans l'Industrie d'Aluminium*, 1st edition, Le Presse d'aluminium (PRAL), **2012**.
- [21] S. Wilkening, J. Côté, J., *Light Metals*, **2007**, p. 865.

## Figure Captions

**GRAPHICAL ABSTRACT** Anode production process and the production steps where the anode cracks form

**FIGURE 1** Production of 24 anodes

(V1, V2, V3, and V4 represent the vibro-compactor 1, 2, 3, and 4, respectively)

**FIGURE 2** Overview of horizontal anode baking furnace <sup>[15]</sup>

**FIGURE 3** Position of anodes in two pits (\*Anodes indicated by (D) are not used in measurement campaign)

**FIGURE 4** Positions of cores in the anodes

**FIGURE 5** Classification of cracks (A) according to zone, (B) according to type

**FIGURE 6** Representation of different possible cracks on the anode

**FIGURE 7** Percent of cracks formed during the vibro-compaction at two different vibration times

**FIGURE 8** Percent of cracks formed during vibro-compaction by different vibro-compactors

**FIGURE 9** Cracked stub holes

**FIGURE 10** Percent of anodes with cracked stub holes and number of stub holes for anodes produced at different vibro-compactors

**FIGURE 11** Distribution of the crack densities in the horizontal direction in anodes

**FIGURE 12** Distribution of the crack density in the vertical direction in anodes

**FIGURE 13** Distribution of crack density according to crack type

**FIGURE 14** Effect of anode position in the baking furnace on anode crack density

**FIGURE 15** Effect of butt content on crack density (F-value = 1.344, F-critical value = 4.590, p-value = 0.399)

**FIGURE 16** Effect of pitch type on crack density (F-value = 1.443, F-critical value = 2.818, p-value = 0.277)

**FIGURE 17** Effect of coke type on crack density (F = 1.443, F-critical value = 2.818, p = 0.277)

**FIGURE 18** Crack density as a function of anode electrical resistivity

## Table Captions

**TABLE 1** Anode production parameters

<b>Anode</b>	<b>Coke</b>	<b>Butt (%)</b>	<b>Pitch</b>	<b>Vibro</b>	<b>Pressure (psi)</b>	<b>Vibration time (s)</b>	<b>Row</b>
1	Coke 1	32	Pitch 1	1	20	30	2
2	Coke 1	32	Pitch 1	1	20	30	3
3	Coke 1	32	Pitch 1	1	20	30	1
4	Coke 2	20	Pitch 2	2	25	30	1
5	Coke 2	20	Pitch 2	2	25	30	3
6	Coke 2	20	Pitch 2	2	25	30	2
7	Coke 1	32	Pitch 1	3	40	30	1
8	Coke 1	32	Pitch 1	3	40	30	2
9	Coke 1	32	Pitch 1	3	40	30	3
10	Coke 2	32	Pitch 2	4	30	30	1
11	Coke 2	32	Pitch 2	4	30	30	3
12	Coke 2	32	Pitch 2	4	30	30	2
13	Coke 1	32	Pitch 1	1	20	37	3
14	Coke 1	32	Pitch 1	1	20	37	2
15	Coke 1	32	Pitch 1	1	20	37	1
16	Coke 2	20	Pitch 2	2	25	37	1
17	Coke 2	20	Pitch 2	2	25	37	3
18	Coke 2	20	Pitch 2	2	25	37	2
19	Coke 1	32	Pitch 1	3	40	37	1
20	Coke 1	32	Pitch 1	3	40	37	3
21	Coke 1	32	Pitch 1	3	40	37	2
22	Coke 2	32	Pitch 2	4	30	37	3
23	Coke 2	32	Pitch 2	4	30	37	1
24	Coke 2	32	Pitch 2	4	30	37	2

**TABLE 2** Properties of pitches

	<b>Pitch 1</b>	<b>Pitch 2</b>
Density at 20°C (g/ml)	1.320	1.320
Softening point, Mettler, (°C)	120.6	121.4
Quinoline insoluble (QI) (% m/m)	7.2	6.9
Toluene insoluble (TI) (% m/m)	29.3	30.3
β-resin	22.1	23.4
Coking value, Alcan (% m/m)	58.4	60.8
Ash at 900°C (% m/m)	0.15	0.2
Dynamic viscosity at 150°C (mPa.s)	13594	12800
Dynamic viscosity at 170°C (mPa.s)	2051	1620
Dynamic viscosity at 190°C (mPa.s)	521	450



**TABLE 3** Properties of cokes

	<b>Coke 1</b>	<b>Coke 2</b>
<b>Real density (g/cm<sup>3</sup>)</b>	2.066	2.065
<b>Apparent density (g/cm<sup>3</sup>)</b>	0.842	0.840
<b>Ash (%)</b>	0.13	0.13
<b>Moisture (%)</b>	0.08	0.02
<b>S (%)</b>	2.37	2.50
<b>Si (g/g)</b>	$6.2 \times 10^{-5}$	$6.2 \times 10^{-5}$
<b>V (g/g)</b>	$3.34 \times 10^{-4}$	$3.51 \times 10^{-4}$
<b>Ca (g/g)</b>	$2.5 \times 10^{-5}$	$3.4 \times 10^{-5}$
<b>Ni (g/g)</b>	$1.84 \times 10^{-4}$	$1.70 \times 10^{-4}$
<b>Fe (g/g)</b>	$9.6 \times 10^{-5}$	$87 \times 10^{-5}$
<b>Na (g/g)</b>	$2.4 \times 10^{-5}$	$1.4 \times 10^{-5}$

**TABLE 4** Anode properties

<b>Anode</b>	<b>Vibro</b>	<b>Vibration time (s)</b>	<b>Row number in furnace</b>	<b>Relative anode density</b>	<b>Relative resistivity</b>	<b>Relative crack density</b>
1	1	30	2	0.998	0.98	0.430
2	1	30	3	1.001	0.95	0.430
3	1	30	1	0.998	1.10	2.099
4	2	30	1	0.989	1.09	1.116
5	2	30	3	0.991	0.94	0.202
6	2	30	2	1.003	0.98	0.984
7	3	30	1	1.008	1.15	2.196
8	3	30	2	1.002	0.97	1.028
9	3	30	3	1.008	0.91	0.264
10	4	30	1	1.010	1.05	2.214
11	4	30	3	0.999	0.89	0.246
12	4	30	2	0.999	0.97	1.116
13	1	37	3	1.001	0.96	0.395
14	1	37	2	0.999	0.96	1.107
15	1	37	1	1.002	1.09	1.836
16	2	37	1	0.982	1.11	1.853
17	2	37	3	0.989	0.93	0.149
18	2	37	2	0.985	0.99	1.792
19	3	37	1	1.015	1.10	3.057
20	3	37	3	1.011	0.93	1.054
21	3	37	2	1.008	0.97	2.170
22	4	37	3	1.002	0.95	0.545
23	4	37	1	0.998	0.97	2.012
24	4	37	2	1.002	1.06	1.818